

# Ability of reflection high energy electron diffraction (RHEED) to observe structural modifications in ion-implanted and annealed GaAs

M. ROSSI, G. VITALI

*Energetics Department, Università degli Studi di Roma "La Sapienza", via A. Scarpa, 14, 00161 Roma, and GNSM of CNR, Roma, Italy*

D. KARPUZOV\*, M. KALITZOVA†

*Institutes of \*Electronics, and †Solid State Physics, Bulgarian Academy of Sciences, Blv. Lenin 72, Sofia 1784, Bulgaria*

H. BUDINOV

*Institute of Micro and Optoelectronics, Botevgrad 2141, Bulgaria*

GaAs  $\langle 100 \rangle$  wafers were implanted and later annealed by using three different techniques: furnace thermal annealing (FTA), flash lamp (RTA) and low-power laser annealing (LPLA). The resulting modifications of the structure were studied by RHEED. The RHEED pattern analysis indicates that: (a) A well annealed structure is observed after thermal treatment in furnace at 850 °C for 30 min; (b) the particular RTA employed leads to some texturing, but is not sufficient to provide good structural effects; (c) best annealing under our conditions is obtained by the LPLA technique, especially for low ion doses (less than  $10^{13} \text{ cm}^{-2}$ ); (d) variable-glancing-angle RHEED is an effective and convenient method to investigate the ion induced disorder in crystals at small depths.

## 1. Introduction

The high speed performance advantages of GaAs devices over Si are well documented [1–4]. GaAs MESFETs and ICs have been extensively investigated as practical low-noise and high power devices for high-frequency applications. They are usually produced by means of direct ion implantation into a crystalline substrate. However, the ion bombardment induced damage must be removed by a suitable post-implantation annealing treatment to achieve a good structural re-ordering and a high efficiency of doping.

In the last few years, some short time and pulsed annealing techniques have been developed to avoid the long heating time involved with the conventional techniques and to obtain the minimal dopant re-distribution. Furthermore, using the traditional techniques, it is necessary to cap the GaAs (i.e., with  $\text{SiO}_2$ ) during the annealing time in order to prevent a surface contamination and a possible alteration of the stoichiometric composition. These alternative techniques can also be useful to avoid the capping step in the manufacturing of the devices. The literature gives various examples of GaAs devices obtained using these techniques [2].

Different analyses, such as electrical and optical measurements, secondary ion mass spectroscopy (SIMS) profiling, Rutherford back-scattering (RBS) and so on, can be carried out to obtain distinct

information on the annealing effects. In any case, the device characteristics are strongly correlated with the structure of the annealed-implanted layers and can be influenced by eventual surface contaminations. Nevertheless, it is not easy to obtain direct information about the crystallographic structure of thin layers near the surface without using destructive techniques, such as Transmission Electron Diffraction (TED).

The central aim of the present work is to verify the capability of RHEED with variable incidence angle, to reveal, in a non-destructive way, eventual surface fine structural modifications in ion-implanted semi-insulating (SI)  $\langle 100 \rangle$  GaAs single crystals after three different annealing treatments: (a) Conventional FTA; (b) RTA using a flash lamp system; (c) LPLA [5].

The implanted doses and energies (Table I) were selected as being typical for the formation of active, as well as,  $n^+$  layers of low-noise SI-GaAs MESFETs.

## 2. Experimental procedure

### 2.1. Ion implantation

Three Series (I, II and III) of  $\langle 100 \rangle$  semi-insulating GaAs wafers were implanted at room temperature and a tilting angle of  $7^\circ$  to avoid channelling effect. High (120 keV) and low (33 keV) energy of  $\text{Si}^+$  were used in Series I and III, respectively. In Series II successive implantation of  $\text{Si}^+$  (120 keV) and  $\text{As}^+$  (280 keV) were

TABLE I Ion-implantation parameters and relative classification of the specimens.

	Ions	Energy (keV)	Dose (ions cm <sup>-2</sup> )
Series I	Si <sup>+</sup>	120	6 × 10 <sup>12</sup>
Series II	Si <sup>+</sup>	120	6 × 10 <sup>12</sup>
	As <sup>+</sup>	280	6 × 10 <sup>12</sup>
Series III	Si <sup>+</sup>	33	10 <sup>14</sup>

carried out to result in approximately equal mean ion projected range. Dose parameters are given in Table I.

## 2.2. Annealing

Before this treatment all samples were covered by 150–180 nm thick SiO<sub>2</sub> grown pyrolytically. The capping is commonly used in GaAs technology to avoid losses of As when the temperature rises over about 450 °C. The various annealings were carried out as follows:

### 2.2.1. Furnace annealing

It was performed in H<sub>2</sub> environment in a furnace at 850 °C for 30 min.

### 2.2.2. RTA

A flash lamp system, consisting of two tubular Xenon lamps [6, 7] was used. The energy density at the wafer surface was 0.75 J cm<sup>-2</sup> per pulse and we irradiated the samples with 100 superimposed pulses ( $\tau = 1$  ms and  $f = 10$  Hz).

### 2.2.3. LPLA

Low-power pulses ( $\lambda = 694.3$  nm) of a Q-switched ruby laser were used to anneal the samples without reaching the melting temperature at the surface, as reported in [5]. We used a JK Laser System (Model 2000) equipped with a suitable optical guide to assure a homogeneous spatial exposure to the beam [5]: on the basis of our results this is one of the main conditions to obtain an effective LPLA. At the estimated temperature (less than 400 °C) an appreciable alteration of the GaAs stoichiometry is not expected and so the presence of a cap layer is superfluous. Furthermore, the SiO<sub>2</sub> film cap partially absorbs the laser energy and in the future we intend to find a way to measure this absorption in the conditions we employed. Therefore we performed LPLA with and without a protective layer and compared the resulting effects. In the latter case the removal of the layer was carried out immediately before the LPLA treatment. More details about the LPLA parameters used will be published elsewhere.

## 2.3. Analysis

The RHEED technique was applied to study the crystal structure of the samples before and after annealing. In all cases, prior to the analysis, the capping

SiO<sub>2</sub> layer was removed by chemical processing. The used system was an EM6G AEI Electron Microscope equipped with a high resolution electron diffraction stage (electron beam energy at 60 keV). Using this stage it is possible to carry out the variable-glancing-angle RHEED technique [8]. The variation of the electron beam incidence angle,  $\theta$ , with respect to the specimen surface, allows the detection of structural changes at different depths in the specimens. It is possible to vary  $\theta$  from the minimum value for the Bragg condition,  $\theta = 0.8^\circ$ , at which the corresponding RHEED pattern refers to the first few atomic layers of the implanted material only (a few nanometres), to a maximum value that depends on the experimental conditions. In our case at  $\theta = 4.5^\circ$  the RHEED pattern refers to layers situated at depths of about 30–40 nm. Varying  $\theta$  slowly between these two values (0.8 and 4.5°), it is possible to record all the structural changes from the surface to these levels and to obtain information on the structure at different depths of the material examined.

By rotation of the specimen around the normal to the surface we could observe diffraction patterns in different azimuth directions.

## 3. Results and discussion

### 3.1. Ion implantation

RHEED patterns of all as-implanted samples reveal diffuse rings typical of amorphous-like structures. Fig. 1a,b,c show the patterns of as-implanted specimens of Series I, II and III, respectively, obtained at  $\theta = 0.8^\circ$ .

### 3.2. Furnace annealing

Furnace annealing results in good structural re-ordering in microcrystallites (mosaic structures), demonstrated by sets of well-expressed diffraction spots from small depths of about 5 nm for different azimuth directions (Figs 2a–c, 3a and 4a). The best regrowth is evident for Series I and azimuth  $\langle 100 \rangle$  (Fig. 2a). Some Debye rings (strong in Fig. 3a and weaker in Fig. 2a) are also observed which do not correspond to polycrystalline GaAs; based on [9, 10] it is reasonable to suppose that these rings are related to the presence of oxides, most probably Ga<sub>2</sub>O<sub>3</sub>. Some residual disorder is still seen as diffuse halos in the patterns. RHEED results for higher incidence angle ( $\theta \approx 4.5^\circ$ , see Fig. 5b) exhibit good crystal structure at layers that, in accordance with [8] we estimated to be at depths  $\geq 30$ –40 nm.

In the samples implanted twice (Series II, see Fig. 3a), according to the characteristics of the diffraction patterns, is present a heavy surface contamination (strong Debye rings) and the re-ordering after the furnace annealing is smaller (weak spots) than in Series I (Fig. 2a,b,c) and III (Fig. 4a). In our opinion, this is due to the presence of heavier ion-induced damage in the series II specimens.

Regarding the last Series (III, Fig. 4), one can note that the furnace annealing (Fig. 4a) leads to appearance of additional set of diffraction spots, with lower

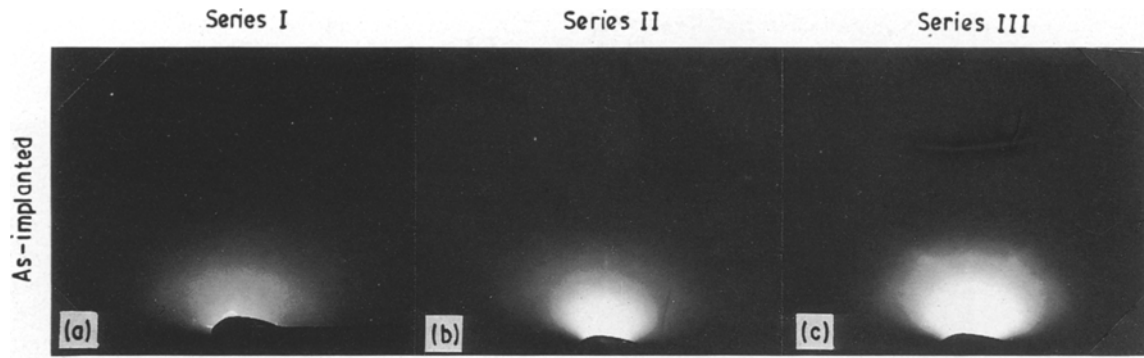


Figure 1 RHEED patterns of as-implanted GaAs specimens of:(a) Series I, (b) Series II and (c) Series III, respectively.

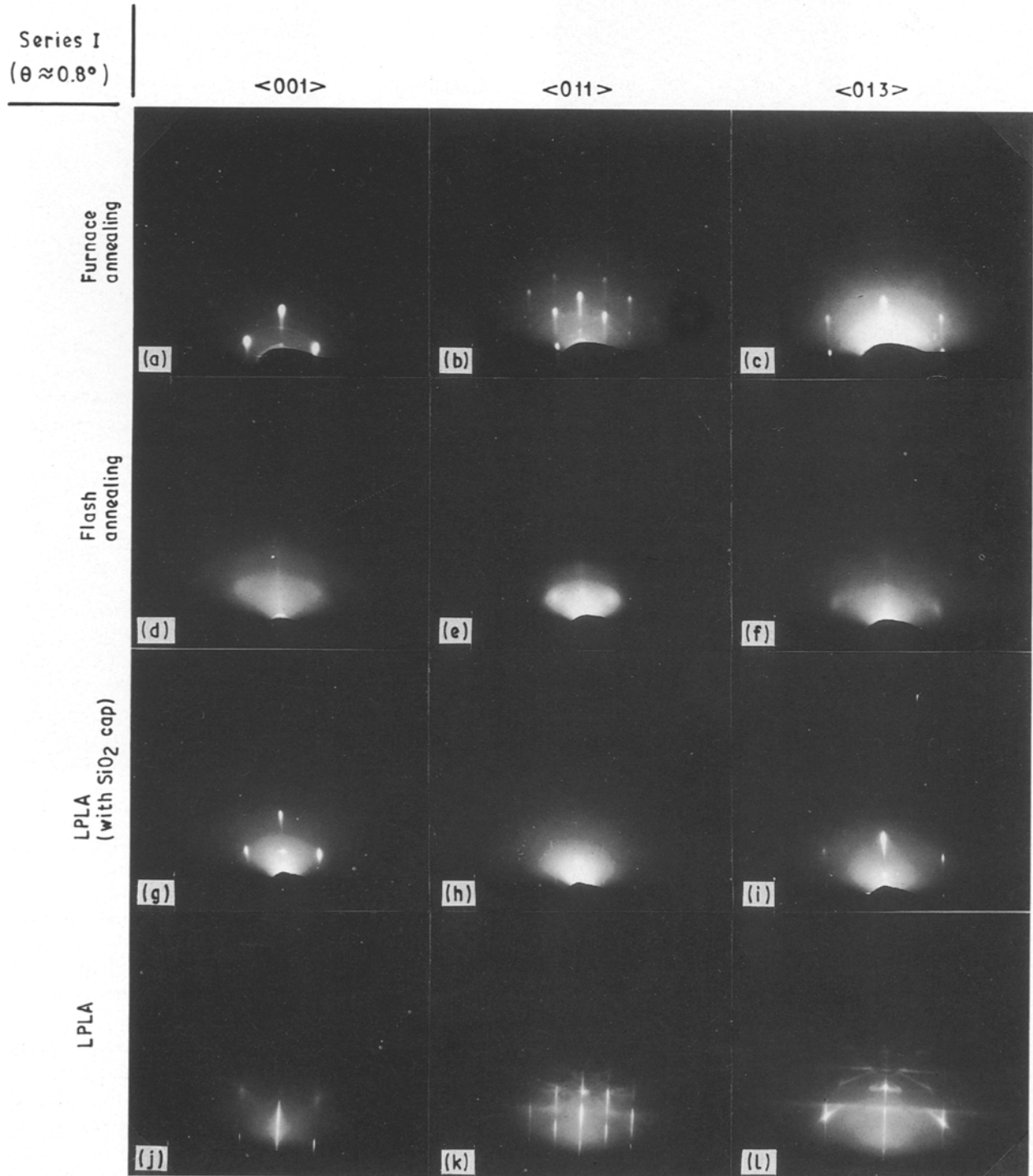


Figure 2 RHEED patterns (with glancing-angle  $\theta = 0.8^\circ$ ) of Series I, GaAs specimens after: FTA (a-c), RTA (d-f), LPLA with (g-i) and without (j-l)  $\text{SiO}_2$  cap. (a), (d), (g), (j) refer to  $\langle 001 \rangle$ , (b), (e), (h), (k) to  $\langle 011 \rangle$  and (c), (f), (i), (l) to  $\langle 013 \rangle$  azimuth directions.

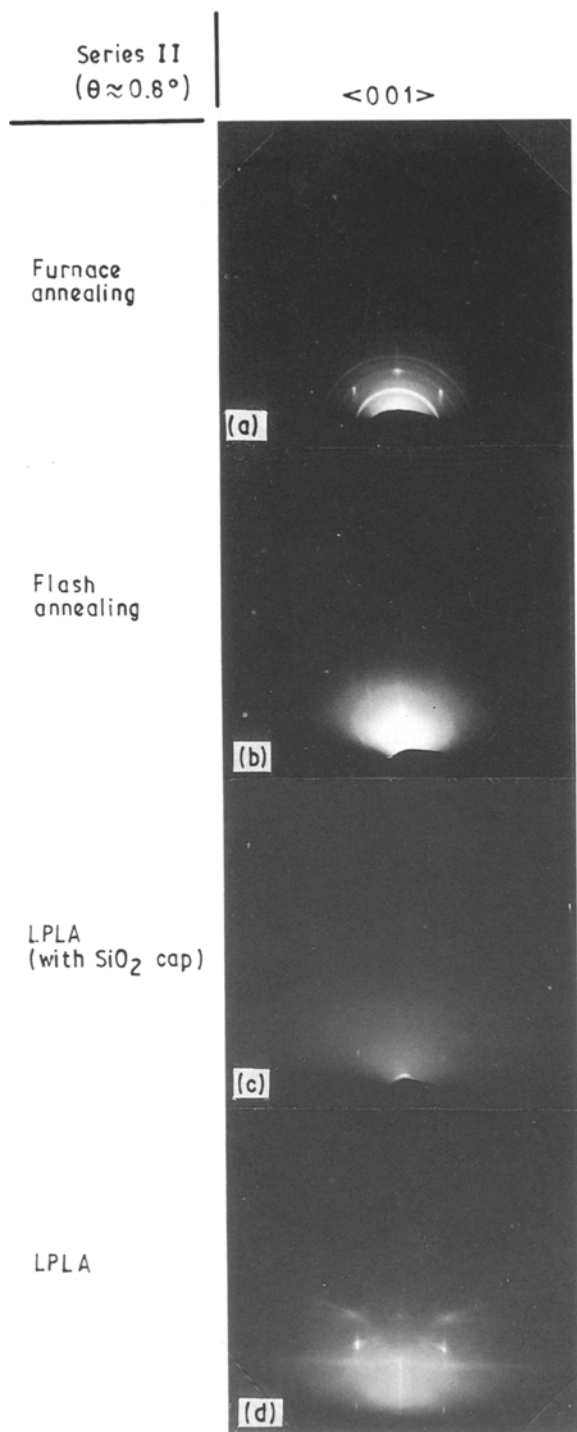


Figure 3 RHEED patterns ( $\theta = 0.8^\circ$ ,  $\langle 001 \rangle$  azimuth directions) of Series II GaAs specimens: (a) after FTA, (b) after RTA, and after LPLA (c) with and (d) without  $\text{SiO}_2$  cap.

intensity compared to that corresponding to the matrix. These spots are located on the Debye rings mentioned above and their utmost intensity is observed in the case of low-energy high-dose implantation (Fig. 4a). It can be concluded that during furnace annealing some crystallization of the surface oxides occurs.

### 3.3. Flash lamp annealing

Flash lamp annealing gives RHEED patterns with very diffused spots. Their intensity and position at

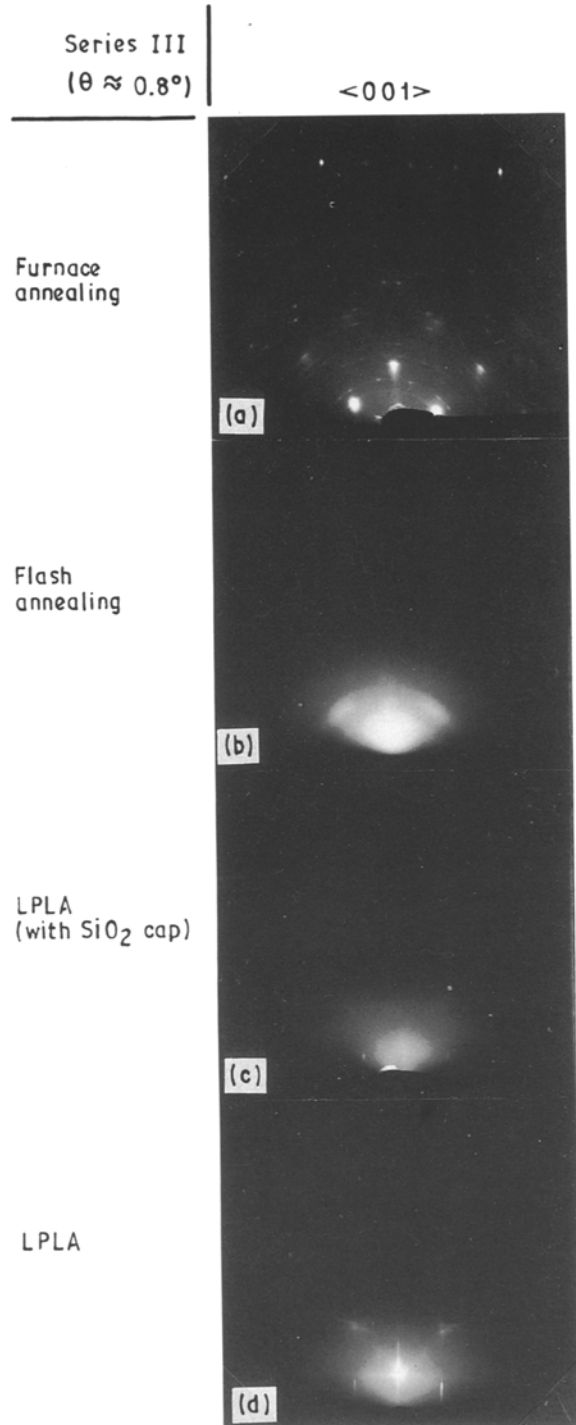


Figure 4 RHEED patterns ( $\theta = 0.8^\circ$ ,  $\langle 001 \rangle$  azimuth directions) of Series III GaAs specimens: (a) after FTA, (b) after RTA, and after LPLA (c) with and (d) without  $\text{SiO}_2$  cap.

different azimuths (Fig. 2d,e,f) allow us to consider that a starting regrowth with preferential orientation (almost like a texture) takes place. The shape of the spots and their intensities indicate that the crystalline grains are of extremely small dimensions.

In the case of double implantation at high energy (Series II, Fig. 3b), when heavy damaging can be expected up to depths of about  $0.1 \mu\text{m}$ , the RHEED analysis does not indicate any recrystallization induced by RTA. In the case of low-energy irradiation, however, where all the damage is near the surface, a tendency to texturing can be found again (Series III, Fig. 4b).

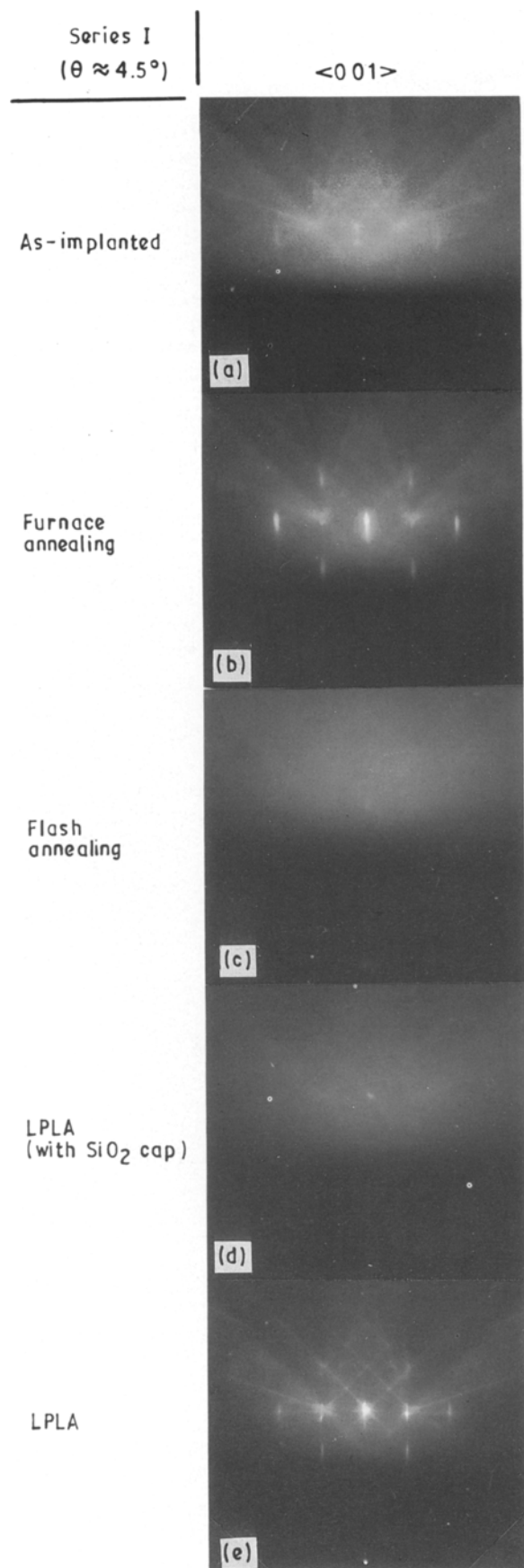


Figure 5 RHEED patterns (with  $\theta = 4.5^\circ$ ,  $\langle 001 \rangle$  azimuth directions) of Series I GaAs specimens: (a) as-implanted, (b) after FTA, (c) after RTA, and after LPLA (d) with and (e) without SiO<sub>2</sub> cap.

### 3.4. Low power laser annealing

Low-power laser annealed samples indicate high quality structural re-ordering (Fig. 2g-1). It is worth noting

that this is the only type of annealing after which heavy surface contamination is not observed.

When the LPLA is carried out on bare specimens (without SiO<sub>2</sub> layer) the RHEED patterns consist of well pronounced high intensity spots and Kikuchi lines for both small ( $\theta = 0.8^\circ$ , Fig. 2j-1) and large ( $\theta = 4.5^\circ$ , Fig. 3e) incidence angles. This fact clearly demonstrates a good quality crystal regrowth through all the depth of the implanted layer. The elongation of the spots can be explained as a consequence of slight distortion of the near surface atomic planes [11].

In the case of LPLA treatment through a protective SiO<sub>2</sub> layer (Fig. 2g-i) one can observe a combination of diffraction spots on the background of an intense diffuse halo. Since the irradiation conditions were the same regardless of the presence or the absence of a SiO<sub>2</sub> cap, we can consider the effect of such protective layer by comparing the corresponding RHEED patterns, i.e., Figs 2g-i, 3c, 4c and 5d, on one side, with Figs 2j-1, 3d, 4d and 5e, on the other. From these results we can conclude that the SiO<sub>2</sub> protective layer has essentially worked as an optical absorber, so that a thin upper layer can be recrystallized only. Beyond the regrown region we again find a buried layer of residual ion-induced disordering, which causes a dominant halo in the pattern (Fig. 5d). In other words, in all events the deposited laser energy, although low, was able to bring structural changes in the top surface layers (Fig. 2g-i). On the contrary, the RHEED analyses of deeper layers show an increase of the disorder (Fig. 5d), compared to as-implanted specimen (Fig. 5a). This effect can be explained if we consider that the deposited laser energy provides a temperature gradient between the surface and the deepest layers. This gradient might cause migration of the defects towards the deepest layers, where they accumulate [12] increasing the local disorder due to ion-implantation.

A similar behaviour is observed in the RTA case (Fig. 5c).

## 4. Conclusions

The unique opportunity of using RHEED technique with variable incidence angle,  $\theta$ , is a convenient non-destructive way to investigate the annealing effects on implantation-induced crystal disorder at different depths. It is extremely suitable for studying the damage in the near-surface layers where the sensitivity of all other techniques is not sufficient. From the results of RHEED analysis one can deduce that:

1. Furnace annealing produces good structural re-ordering throughout the implanted layer, but enhances the Ga-oxidation in the top (about 5 nm) surface region.
2. The particular RTA processing used is not effective in the annealing of GaAs samples implanted in accordance with the Table I.
3. Under the LPLA conditions, the RHEED analysis points out two different effects depending on the deposited energy:
  - (a) At very low energies, comparing to melting threshold, the prevalent effect seems to be an increasing of the disorder in the deep implanted layers;

(b) at higher energies (but always below the melting point) the structural annealing occurs not only on the surface, but in the deeper layers too.

Under our conditions the LPLA proves to be the most effective technique for treatment of ion-implanted GaAs, when the protective SiO<sub>2</sub> layer is removed. In this case, a high-quality recrystallization is observed through all the depth of the implanted layer. In SiO<sub>2</sub> capped samples the laser power used is not sufficient to recrystallize the whole damage induced by implantation.

### Acknowledgements

The authors wish to thank Professor N. Pashov for his helpful suggestions and discussions concerning the present work. This work has been carried out within the framework of the scientific agreement between the Italian CNR and the Bulgarian Academy of Sciences.

### References

1. A. G. ROPER and J. G. ROPE, *Solid State Technol.* **28** (1985) 209.

2. P. M. ASBECK, D. L. MILLER, R. J. ANDERSON and E. M. EISEN, *IEEE Electron Devices Lett.* **EDL-5** (1984) 310.
3. H. KANBER, W. B. HENDERSON, R. C. RUSH, M. SIRACUSE and J. M. WHELAN, *Appl. Phys. Lett.* **47** (1985) 120.
4. T. MAZUTANI, K. ARAI, K. OE, S. FUJITA and F. JANAGAWA, *Elect. Lett.* **21** (1985) 638.
5. G. VITALI and G. CREA, *Vacuum* **36** (1986) 643.
6. H. BUDINOV, R. BURKOVA and I. BALTOV, in Proceedings of the Second International School "New materials and technologies" (Primorsko, Bulgaria, 1986) p. 263.
7. H. BUDINOV, V. STAVROV and R. BURKOVA, *Phys. Status Solidi A*, **114** (1989) K131.
8. G. VITALI, M. BERTOLOTTI, U. ZAMMIT and M. MARINELLI, *Phys. Letts.* **89A** (1982) 199.
9. C. J. BULL and B. J. SEALY, *Phil. Mag.* **37** (1978) 489.
10. M. HALL, M. F. RAU and J. W. EVANS, *J. Electrochem. Soc.* **133** (1986) 1934.
11. L. A. ZHUKOVA and M. A. GUREVICH, in "Electronografia poverkhnostnykh sloev i plenok poluprovodniakovykh materialov" (Metallurgizdat, Moskva, 1971) p. 71.
12. G. VITALI, M. MARINELLI, U. ZAMMIT and F. SCUDIERI, *Phys. Letts.* **94A** (1983) 320.

*Received 15 January*

*and accepted 16 May 1990*